Trabajo de Fin de Grado:

INTRODUCTION TO SOLAR SPECTROPOLARIMETRY

David Afonso Delgado

Tutor: Basilio Ruiz Cobo

Universidad de La Laguna

Grado en Física

Contents

ABSTRACT.

Spectropolarimetry is one of the most powerful techniques to study the magnetic structures in the Sun. Specially, the spectropolarimetry has been very useful to increase our knowledge about sunspot, these structures have the higher magnetic field in the Sun so, the study of the polarized light is essential to understand their formation and evolution.

Using a code able to synthesize Stokes spectra from a model atmosphere (the SIR code), we have studied how changes of several physics variables (temperature, magnetic field strength, inclination and azimuth, and the velocity of the plasma) affect the Stokes profiles (I, V, U and Q). We have applied this knowledge to study a set of real data, in particular the Stokes spectra of two photospheric iron lines observed in an active region including a big sunspot. The data were taken by the spectropolarimeter SP on board of the Japanese satellite Hinode. This allowed us to identify and analyze some photospheric structures, such as the umbra and the solar granulation. Also, we have applied two simple approaches in order to obtain two maps of the variation of temperature and line-of-sight component of the velocity from the observe data. The results allow us to confirm the convective character of the solar granulation.

RESUMEN.

La espectropolarimetría es una de las técnicas más poderosas para el estudio de las estructuras magnéticas en el Sol. La espectropolarimetría ha sido especialmente útil para aumentar nuestro conocimiento sobre las manchas solares. Estas estructuras tienen los mayores campos magnéticos en el Sol y, por lo tanto, el estudio de la luz polarizada es esencial para entender su formación y configuración.

A través de un código capaz de sintetizar el espectro de Stokes a partir de un modelo de atmósfera (el código SIR), hemos estudiado como los cambios de ciertas variables físicas (temperatura, intensidad, inclinación y azimut del campo magnético y velocidad del plasma) afectan a los perfiles de Stokes (I, V, U y Q). Aplicamos este conocimiento para estudiar un conjunto de datos reales, en particular el espectro de Stokes de dos líneas de hierro formadas en una zona activa de la fotosfera que incluye una mancha solar de gran tamaño. Los datos fueron tomados con el espectropolarímetro SP a bordo del satélite japonés Hinode. Nos permitió identificar y analizar algunas de estructuras presentes en la fotosfera, como la umbra y la granulación solar. También aplicamos dos simples aproximaciones con el objetivo de obtener dos mapas de las variaciones en temperatura y de la velocidad en la línea de visión a partir de los datos observacionales. Los resultados nos permiten confirmar el carácter convectivo de la granulación solar.

1. INTRODUCTION.

La fotosfera del Sol presenta dos estructuras características de gran interés. Las manchas solares con una temperatura mucho menor que la temperatura media de a fotosfera y la presencia de campos magnéticos de gran intensidad. Y la granulación, que cubre la mayor parte de la superficie del Sol y que es la manifestación del movimiento de convección que sucede bajo a superficie de la fotosfera.

Además, introducimos varios conceptos físicos que serán necesarios en el avance del trabajo: los parámetros de Stokes necesarios para trabajar con luz polarizada, el desdoblamiento de las líneas espectrales en presencia de un campo magnético que conocemos como efecto Zeeman, y la Ecuación de Transporte Radiativo que nos da evolución de la radiación (en función de los parámetros de Stokes) al interactuar con la materia a lo largo de una capa y en presencia de un campo magnético.

In this first chapter, we are going to introduce some of the theoretical concepts we will need in the work. The material presented in this chapter has been extracted from Stix (2002).

1.1 GRANULATION.

When we observe the Sun with images with high spatial resolution, it is possible to observe a cellular pattern that covers all the surface of the Sun, except for the sunspots. There are many bright elements, called *granules*, which are surrounded by a dark network usually called *intergranules* or intergranular lanes.

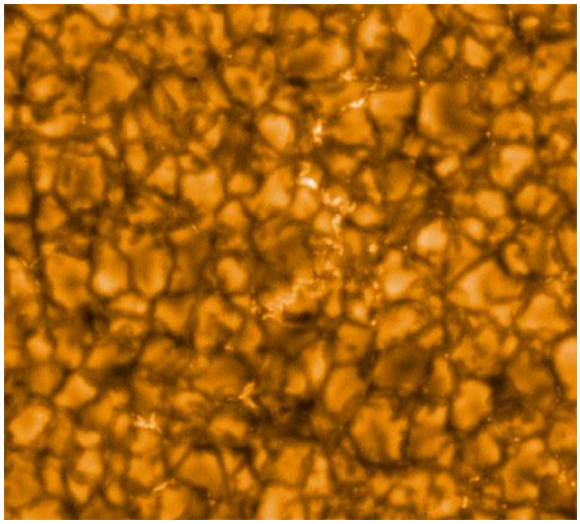

Figure 1. Image of the granulation taken by the satellite HINODE.

Bright granules consist on parcels of hot of plasma moving upwards, at the same time that the darker intergranules harbor cooled downwards-moving plasma. These spatial fluctuations of temperature and velocity produce an observable effect on photospheric spectral lines: mainly, the spectral lines observed in a granule will appear blue-shifted (Doppler effect) while those observed on a intergranule will appear red-shifter. The vertical velocities measured reached the 1.5 km/s. The solar granulation is produced as consequence of convective motions just under the solar surface (Stix, 2002).

The granulation is a system in constant evolution. Most of the granules have their origin in the fragments of the disintegration of older granules. A typical granule evolves growing in size and frequently (explosives granules) it develops a dark spot in the center, that later connects with the intergranules. Finally, the granule splits up forming new fragments that will be the origin of other granules. The mean lifetime of the granules is approximately 6 minutes.

1.2 SUNSPOTS.

Sunspots are structures in the photosphere of the Sun that can be identified as darkenings in some zones of the solar disc. Sunspots can remain in the photosphere between some days and a few months, and have an extension that, varying during their life, is between 1500 and 50000 km.

Sunspots are cooler regions created by the presence of an intense magnetic field (2000-3000 G). Due to the high conductivity of the plasma, the material can only move along the magnetic field lines (Alvèn theorem). Consequently, the presence of a magnetic field inhibits convective motions producing these cold -dark- structures. The temperature in the spot descends until the 3000-4500 K (compared to the 5700-5800 K of the surrounding photosphere).

The magnetic field in the Sun evolves following a 22-years cycle. In one of the phases the magnetic field is stored bellow he convection zone un huge toroidal tubes. As the presence of magnetic field produces a magnetic pressure, these tubes have a lower gas pressure, and consequently a lower density. That situation is unstable and, eventually, these tubes develop loops which ascend, crossing the photosphere and creating a dipolar structure.

Sometimes, a leg of the loop is decomposed in multiple weak tubes, in this case the sunspot looks like a monopole, i.e., ony a single spot is observed.

Sunspots are divided into two zones, the umbra and the penumbra. The umbra is the central zone of the sunspot, it is the darkest one, with a 20% of the quiet photosphere luminosity, and a temperature lower than 4500 K. Here, the magnetic field is more intense (above than 2000 G) and practically perpendicular to the solar surface.

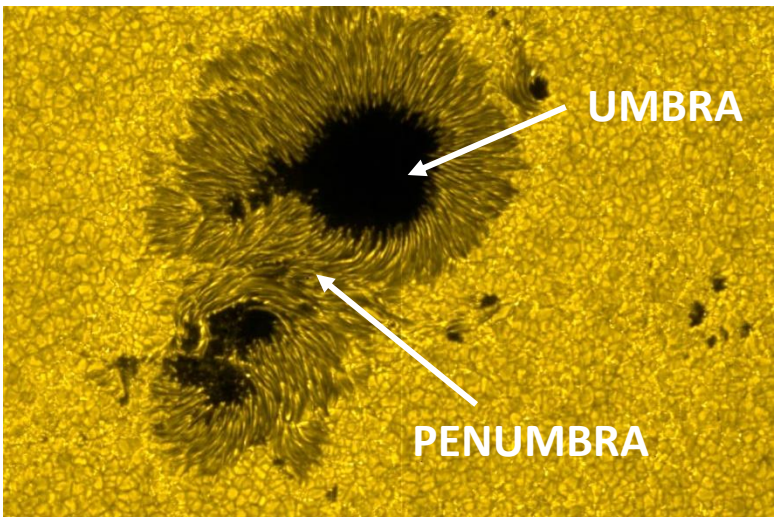

Figure 2. Example of a sunspot.

The penumbra is the part that surrounds the umbra. It reaches the 75% of the luminosity of the quiet Sun, brighter than the umbra, and its temperature is around 5500 K. In this zone, the magnetic field is lower than the umbral one, between 1000 and 2000 G, and the magnetic field vector is nearly horizontal (parallel to the solar surface). Sunspot penumbra is constituted by bunches of dark and bright filaments arranged radially (from the umbra). These filaments are associated with a radial flow from the umbra to the exterior of the sunspot (Evershed effect).

With these definitions, a classification of the sunspots can be presented. This classification is known as Zürich Classification and presents 7 different groups:

- *Group A:* a single spot or a group of spots, without a clear penumbra or a visible configuration of a dipole.
- *Group B:* a group of spots without penumbra. These groups are dominated by two spots that define the group magnetic polarity, which means that the group has a very marked dipolar configuration.
- *Group C:* dipolar groups like the previous one but now one of the principal spots have a zone of penumbra.
- *Group D:* like the previous one but now the two spots present a penumbra. The group extends in less than 10º on the surface of the Sun.
- *Group E:* dipolar groups that occupy more than 10º of the solar Surface. The two principal spots have penumbra and are surrounded by many spots of lower size.
- *Group F:* big size and complexity. Dipolar groups span more than 15º.
- *Group G:* groups spanding more than 10º in the solar surface but the smallest spots between the two principal ones have disappeared.
- *Group H:* monopolar spots with penumbra and a size higher than 2,5º.
- *Group I:* like the previous but now less than 2,5º.

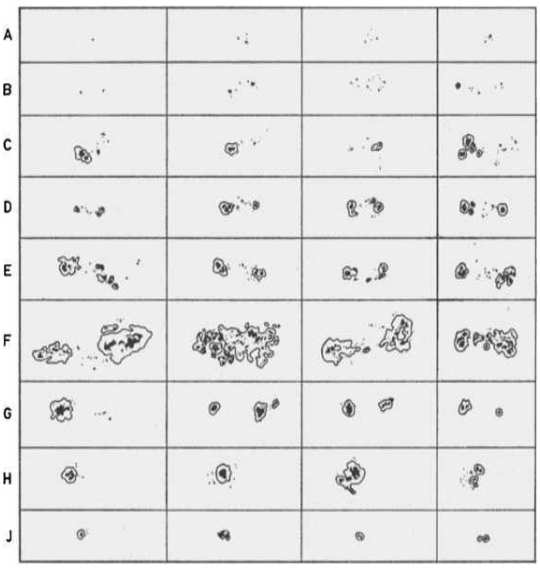

Figure 3. Table with examples of the different groups of sunspots in the Zürich Classification.

The last three groups represent the last steps in the evolution of the sunspots until the sunspot complete disappearance.

1.3 POLARIZED LIGTH AND STOKES PARAMETERS.

The polarized light can be described (Hecht, 1998) with the *Stokes vector*:

$$\vec{I} = \begin{pmatrix} I \\ Q \\ U \\ V \end{pmatrix} \quad (1)$$

In this vector, I gives information about the total intensity, Q and U about the linear polarization and V informs about the amount of circular polarization. In more detail:

- I represents the sum of the intensities of the two components of the electric field that are transmitted through perfect linear polarizers with two perpendicular transmissions axes.
- Q show the difference in intensity between these two linear polarizers.
- U is the difference between two linear polarizers that are at 45º respect to the previous ones (used to define Q).
- V represents the difference between the intensities transmitted through a quarterwave plate followed by two linear polarizers at 45º and 135º. With these definitions, V measures the difference between right (clockwise) and left (counterclockwise) circularly polarized light.

It is possible to do a mathematical description of the Stokes parameters for a monochromatic wave with the electric field amplitudes in the perpendicular plane to the direction of propagation. The components x and y can be expressed as:

$$E_x(t) = \vec{\imath}E_{0x}(t)\cos[(\vec{k}z - \vec{\omega}t) + \varepsilon_x(t)] \quad (2)$$

$$E_y(t) = \vec{\jmath}E_{0y}(t)\cos[(\vec{k}z - \vec{\omega}t) + \varepsilon_y(t)] \quad (3)$$

Where k is the wave number, ω the frequency and ε_x and ε_y the phase in each component.

If we define ε like the difference between the phases of both components, $\varepsilon = \varepsilon_x - \varepsilon_y$, we can express the Stokes parameters in function of the electric field amplitudes (in the expressions, ⟨ ⟩ designate the temporal main value):

$$\begin{aligned} I &= \langle E_{0x}^2 \rangle + \langle E_{0y}^2 \rangle \\ Q &= \langle E_{0x}^2 \rangle - \langle E_{0y}^2 \rangle \\ U &= \langle 2E_{0x}E_{0y}cos\varepsilon \rangle \\ V &= \langle 2E_{0x}E_{0y}sin\varepsilon \rangle \end{aligned} \quad (4)$$

If we analyze the expressions we can deduce the relation:

$$I \geq Q + U + V$$

In the case of not polarized light $\langle E_{0x}^2 \rangle = \langle E_{0y}^2 \rangle$ and the temporal average of $cos\varepsilon$ and the $sin\varepsilon$ are Zero, we obtain: $Q = U = V = 0$ y $I = 2\langle E_{0x}^2 \rangle$.

In the other hand, when we work with completely polarized light the previous equality is fulfilled, so: $I = Q + U + V$.

1.4 ZEEMAN EFFECT.

The Zeeman effect, described for the first time in 1897 by Pieter Zeeman, studies the splitting of a spectral line into several components when the source is in presence of a static magnetic field. Also, it was observed that the magnetic field affects the polarization of the light.

The classical explanation (see for instance Bellot Rubio, 1998 or Ruiz Cobo 1992),

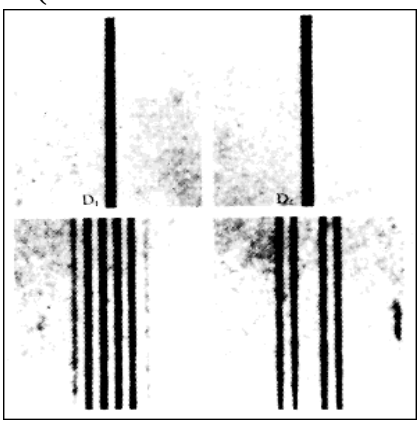

Figure 4. Example of the split in two spectral lines. Anomalous Zeeman effect.

of the Zeeman effect, based on the Lorentz`s theory of the electron, assumes that the oscillation of an electron (with frequency ν_0) is perturbed in the presence of a magnetic field **B**. The new oscillation can be represented by three components: $\nu_0 - \nu_L$, ν_0 and $\nu_0 + \nu_L$ where we introduce the Larmor frequency: $\nu_L = \frac{eB}{4\pi m_{ec}}$. The central component keeps its natural frequency and the direction of the magnetic field **B** (the π-component). The frequencies $\nu_0 \pm \nu_L$ are circular components perpendicular to the direction of propagation (σ-components). The spectral lines are produced by bound-bound transitions i.e., by the absorption (and emission) of a photon as a consequence of a jump of an electron between two bound levels. In the presence of a magnetic field these levels split in several sublevels of different energy, in such a way that in a classical point of view an electron in a given sublevel oscillates with one of the previous frequencies. Consequently, the emitted photon will become circular polarized and with a different frequency, depending of the energy of the sublevels: i.e. one photon will become circular polarized with a frequency $\nu_0 + \nu_L$ and the other counterclockwise, now with frequency $\nu_0 + \nu_L$. The third component is linearly polarized and has a frequency $\nu 0$. In another case, if we look perpendicular to the direction of **B** we are going to see linear polarization perpendicular to **B** at frequency ν_0 and linear polarization parallel to **B** in the frequencies $\nu_0 \pm \nu_L$. This effect is what we name *normal Zeeman effect.*

Some lines in presence of a magnetic field split into four or more components, in these cases we will talk about *anomalous Zeeman effect*, for this effect does not exist an explanation in the classical theory and we need to make a quantum mechanical description of the process of atomic absorption.

In the quantum mechanical description we represent different states in a base $\{\vec{S}^2, \vec{L}^2, \vec{J}^2, J_z\}$ with quantum number $|S,L;J,M>$ (these numbers describe the spin, the orbital angular moment, the total angular moment and the third component of the total angular moment or magnetic moment). The effect of the magnetic field in this representation will be to change the energy of the state, this means to break the degeneration, in function of the values of the number M. Also, the polarization of the photon produced in each transition is well defined with the difference between the value of M in the states of the transition.

We will use the notation S_k, L_k, J_k and M_k with k = 1,2 for the levels up and down in the transition (k=1 the level with more energy, and k=2 the less energetic. For the transitions, we are going to consider in this work exist the rules of selection $\Delta J = 0, \pm 1$ and $\Delta M = 0, \pm 1$.

A transition between states with $\Delta M = 0$ will produce a light linearly polarized, the π-component. If $\Delta M = 1$ the photon will have an elliptic left polarization, σ_b-component. Lastly, with $\Delta M = -1$ we obtain an elliptic right polarization σ_r-component.

So, if λ_0 stands for the wavelength of the transition without a magnetic field, each of the components produced by the split in the Zeeman effect is given by:

$$\Delta\lambda_i = \frac{e\lambda_0^2}{4\pi m_e c^2}(M_1 g_1 - M_2 g_2)_i B \tag{5}$$

Where B denotes the intensity of the magnetic field and the subindex i stands for each component that the split produces. The g coefficients are the Landé factors produced in the interaction spin-orbit of the electron in the atom and can be described as:

$$g_k = \begin{cases} \frac{3}{2} + \frac{S_k(S_k+1) - L_k(S_k+1)}{2J_k(J_k+1)} & if \quad J_k \neq 0 \\ 0 & if \quad J_k = 0 \end{cases} \tag{6}$$

With k = 1,2.

Finally, due to the effects of widening of the spectral lines (thermal motions of the atoms, collisions between the atoms and effects of turbulence), it is difficult to see the fine structure of the Zeeman effect. For this reason, we can group all the transitions in just three components: a not displaced π-component and the two σ-components displaced symmetrically. We can redefine the difference between the wavelengths of components π and σ (with the value of the constants, $\Delta\lambda$ in mÅ, λ_0 in Å y B in Gauss):

$$\Delta\lambda = 4.6685 \times 10^{-10} g_{eff} \lambda_0^2 B \tag{7}$$

Where g_{eff} is the effective Landé factor, that indicates the sensitivity of a spectral line to the magnetic field.

1.5 THE RADIATIVE TRANSFER EQUATION.

The radiative transfer equation (RTE) defines how the Specific Intensity, i.e. the radiation field, evolves after interacting with the matter inside a given layer. In the presence of a magnetic field (or if we take into account the effect of the scattering) it is

needed to modify this equation in order to consider how the Stokes vector evolves after crossing a given layer. It is not the purpose of this work to resolve in detail the RTE, but following the work of Bellot Rubio (1998) we can show some interesting results that will be important in the next chapters.

The first step, is to define the vector of Stokes parameters like in equation (1), the total absorption matrix *K* (a 4x4 matrix describing the absorption properties of the solar atmosphere) and the source function vector which, in analogy with the Stokes vector, can be define as:

$$\vec{S} = \begin{pmatrix} s_I \\ s_Q \\ s_U \\ s_V \end{pmatrix} \tag{8}$$

If we assume a plane-parallel atmosphere, the RTE takes the form:

$$\frac{\mathrm{d}I(z)}{\mathrm{d}z} = -K(z)[I(z) - S(z)] \tag{9}$$

In a magnetic medium, the absorption matrix has some properties of symmetry and, with only seven independent parameters, takes the next expression:

$$K = \begin{pmatrix} \eta_I & \eta_Q & \eta_U & \eta_V \\ \eta_Q & \eta_I & \rho_V & -\rho_U \\ \eta_U & -\rho_V & \eta_I & \rho_Q \\ \eta_V & \rho_U & -\rho_Q & \eta_I \end{pmatrix} \tag{10}$$

Here η_I describes the absorption of the radiation regardless of its polarization state. η_Q, η_U and η_v the coupling of the intensity I with the component Q, U and V due to absorption. And the terms ρ_Q, ρ_U and ρ_V the crosstalk between the polarized components Q, U and V.

To make a mathematical description of the absorption matrix elements we need first assume some hypothesis:

- We are working in regimen of strong magnetic field, this means $B \gg W_{SO}$, where W_{SO} represents the interaction spin-orbit of the electron. In this case doesn´t exist interferences between sublevels when the Zeeman effect is applied.
- Atomic polarization must be negligible. This condition means that the collisional rates are high enough, which ensures that the various sublevels to the same energy are equally populated.
- The frequency and direction of photons scattered are independent of the direction and frequency of incomings electrons.

Under these conditions, the elements of the absorption matrix are:

$$
\begin{aligned}
\eta_I &= k_C + \frac{1}{2}k_l\left[\eta_b \sin^2\gamma + \frac{\eta_b+\eta_r}{2}(1+\cos^2\gamma)\right] \\
\eta_Q &= \frac{1}{2}k_l\left(\eta_p - \frac{\eta_b+\eta_r}{2}\right)\sin^2\gamma\cos 2\chi \\
\eta_U &= \frac{1}{2}k_l\left(\eta_p - \frac{\eta_b+\eta_r}{2}\right)\sin^2\gamma\sin 2\chi \\
\eta_V &= \frac{1}{2}k_l(\eta_r - \eta_b)cos\gamma \\
\rho_Q &= \frac{1}{2}k_l\left(\rho_p - \frac{\rho_b+\rho_r}{2}\right)\sin^2\gamma\cos 2\chi \\
\rho_U &= \frac{1}{2}k_l\left(\rho_p - \frac{\rho_b+\rho_r}{2}\right)\sin^2\gamma\sin 2\chi \\
\rho_V &= \frac{1}{2}k_l(\rho_r - \rho_b)cos\gamma
\end{aligned}
\qquad (11)
$$

Where the subindex p, r and b represent the components π and σ to right and left respectively. To describe the magnetic system we use, in all the work, the next system of coordinates, where the z axes is directed towards the observer.

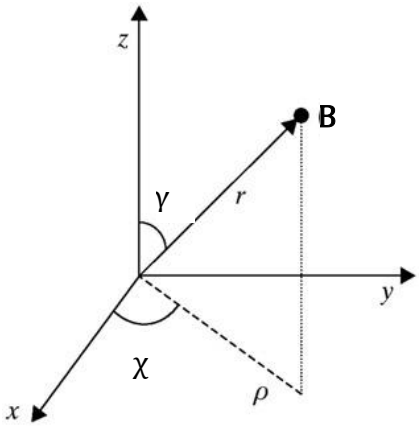

2. SYNTHESIS OF POLARIZED LINES IN FUNCTION OF PHYSICAL PARAMETERS.

A partir del código SIR podemos sintetizar el espectro de Stokes a partir de un modelo de atmósfera solar. Observamos el efecto que tienen sobre los perfiles de Stokes (I, V, U y Q) de una línea de FeI la variación de algunas magnitudes físicas como temperatura, intensidad, inclinación y azimut del campo magnético y la velocidad en la línea de visión del plasma.

In this section, we are going to analyze the variations suffered by the Stokes profiles when some physical parameters are varied. In special, we will study the response of one spectral line of FeI (the line at 6302.49 Angstrom, with a high Landé factor and so, very sensitive to the magnetic field) to variations of temperature, magnetic field vector, or line of sight velocity at photospheric layers (where this line is formed).

In the synthesis, we use SIR (Stokes Inversion based on Response function, Ruiz Cobo & del Toro Iniesta, 1992). SIR is a package for the synthesis and inversion of spectral lines formed in the presence of a magnetic field. In the synthesis mode, the code calculates the Stokes spectra (I, V, U and Q), from a given model of solar atmosphere. This is done by numerically solving the RTE that we presented in (eq. 9). To more information you can see Ruiz Cobo & del Toro Iniesta (1992) and Bellot Rubio (2003).

In order to study the dependence of the Stokes parameters to changes of different physical quantities we have used the VALC model (Vernanza, 1981), after changing by a constant either its temperature, magnetic field (strength, inclination or azimuth) or line of sight velocity.

2.1 TEMPERATURE.

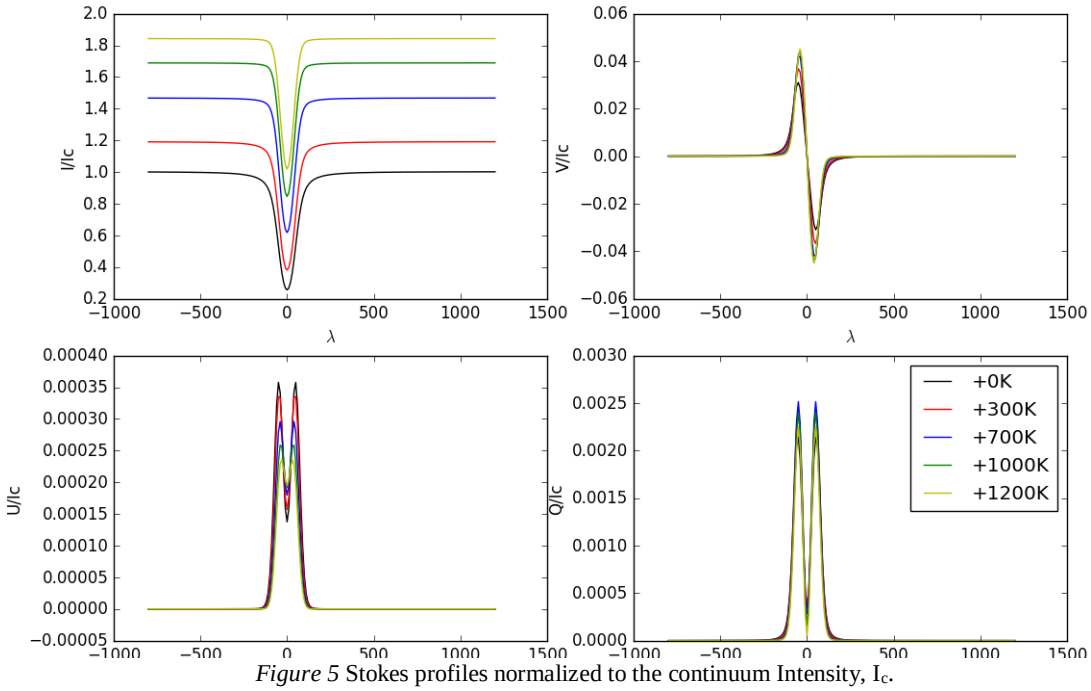

Figure 5 Stokes profiles normalized to the continuum Intensity, I_c.

In this first step, we are going to analyze the changes in the Stokes profiles when we vary the temperature in the solar surface. We show five profiles synthetized after increasing the temperature by 0, 300, 700, 1000, and 1200 K. Also, we kept the magnetic field constant, at a field strength of 300 G an inclination γ of 45º and azimuth χ of 0º. In this configuration, none profile is null.

We can observe that the I profile suffer strong changes when we increase the temperature. On one hand, we can see an increase of the continuum intensity, Ic produced by an increase of the number of bound-free and free-free photons. This effect is produced by an increase of the source function, which is approximately the Planck function evaluated at the temperature of $\tau = 1$ (the bottom of the photosphere). On the other hand, the equivalent width of the line (the area of the depression introduced by the spectral line once we have normalized to the to the continuum) diminishes when the temperature grows. The reason of this is that this is a neutral line (FeI), so the number of neutral iron atoms absorbing photons is lower when the ionization increases (Gray, 1992).

In our case (remember we are working with the FeI line at 6302 Angstroms), the Fe I is almost completely ionized: only between the 2% and 5% are Fe I and between the 98% and 95% are in form of FeII. In these conditions, when we increase the temperature the Fe I will be ionized in FeII so, the population of FeI descends and the spectral line will be less deep.

Other effect is the change of the broadening of the line due to the change of the thermal velocity of the atoms (Doppler width). When the temperature is higher the thermal velocity of the atoms increases (it is proportional to the square root of T). But this effect is too small to be appreciated in the figure, because the dependence of the size of the line with T introduced by the ionization is clearly dominant.

The other Stokes parameters change only when the number of photons increase or diminish. As an example, we can evaluate the amount of right or left circular polarized light, I_r and I_l respectively. As $V = I_r - I_l$ and $I = I_r + I_l$ we can evaluate $I_r = \frac{I+V}{2}$ and $I_l = \frac{I-V}{2}$. Doing that we can see that these profiles are equal to half of stokes I one it is shifted to the right (or left) by an amount that depends only on the magnetic field. But I_r (and I_l) changes with temperatures in the same way that I does.

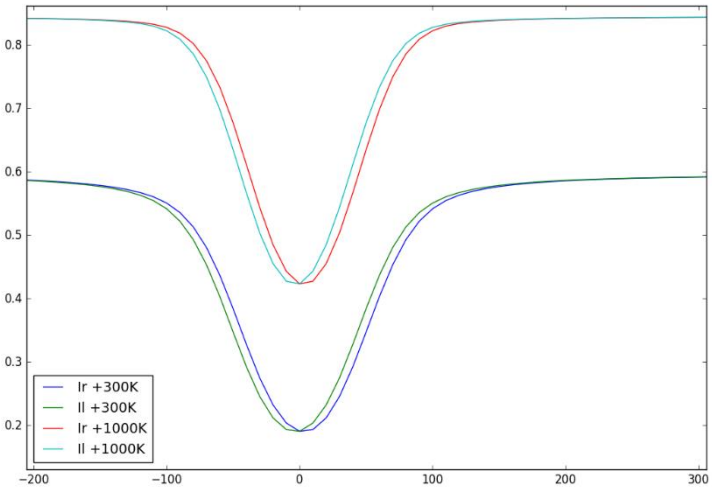

Figure 6. Right and left polarization (I_r and I_l) at 300 K and 1000 K.

2.2 MAGNETIC FIELD STRENGTH.

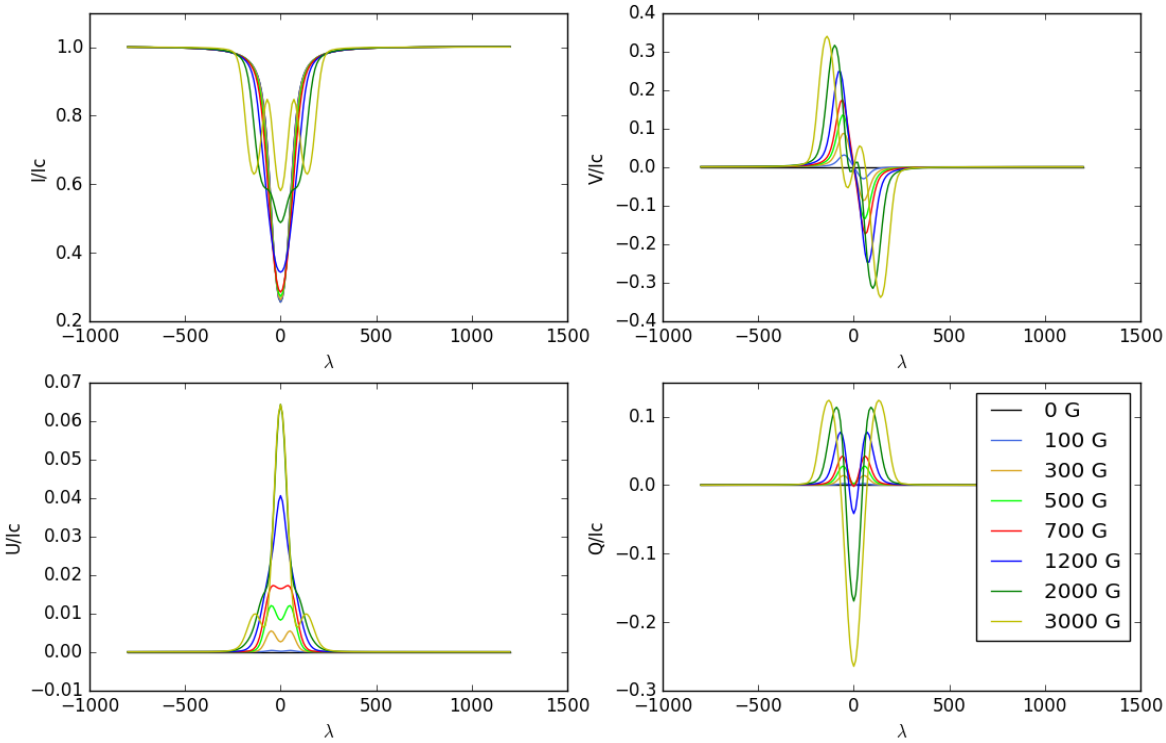

Figure 7. Stokes profile normalized with the continuum intensity Ic with magnetic field strength between 0 and 3000 G.

Now, in this section we are going to keep the temperature, the inclination and azimuth of the magnetic field constant and to vary the magnetic field strength. We are going to study the effect of magnetic field intensity in an interval between 0 and 3000. In this range, we can distinguish two regimes, a strong magnetic field regime (lower than 1200 G) and a strong field regime to fields strengths of 2000 and 3000 G in our study.

In Solar Physics, the term strong field approximation it is used when the two peaks of Stokes V are clearly separated, i.e., when the distance between both peaks is clearly larger than the width of each component. In this case it is possible to obtain the magnetic field directly measuring the distance between peaks (see for instance Stix, 2002). In the other hand, the weak field approximation consists on a series expansion of I+V and I-V as a function of the Zeeman splitting (see for instance Stenflo, 1985). This approximation is valid when the Zeeman splitting (eq. 7) is very small compared with the Doppler width of the line. In this case we can retain only the first term in the Taylor expansion of I+V and I-V. Following the work of Stenflo we define the amount of right and left circular polarized light as $I_r = \frac{I+V}{2}$ and $I_l = \frac{I-V}{2}$ also, if the field is homogenous eq. 7 is vailid and we define these components as:

$$I_{r,l} = \frac{1}{2} I(\lambda \pm \Delta\lambda) \tag{12}$$

So, the V component can be written as:

$$V = \frac{1}{2}(I(\lambda + \Delta\lambda) - I(\lambda - \Delta\lambda)) \tag{13}$$

And if we do a Taylor expansion in function of the Zeeman splitting we obtain:

$$\boldsymbol{V = \Delta\lambda\left[\frac{dI}{d\lambda} + \frac{1}{6}(\Delta\lambda)^2\frac{d^3I}{d\lambda^3} + \cdots\right]} \quad (14)$$

We can conclude that V is proportional to the Zeeman splitting times the derivative of I with respect to λ.

This is to say, in the weak field approximation, the peaks of Stokes V are always in the same position and its size increases linearly with the field. This fact it is used to have a measurement of the magnetic field, simply by calibrating the Stokes V size (this is the rationale behind the magnetogram technique). It is important to clarify that the weak/strong field approximations are valid depending on the ratio between the Zeeman splitting and the Doppler width. This ratio depends on $\frac{Bg\lambda^2}{\lambda\sqrt{T}}$, i.e., for a given B the weak field approximation will be valid for lines with a very small Landé factor, g, and for small wavelength, lambda. On the other hand, the strong field regime will be easily reached for larger wavelengths (for instance in the infrared region of the spectrum).

Now, we are going to start the analysis of Stokes profiles. When the magnetic field B is 0 G, the lines V, U *and* Q are null, as we can see in black in figure 7. As a consequence of the Zeeman effect, non-null Stokes profiles will appear in presence of a magnetic field, *B*.

As we said before, we can distinguish two regimes in the behavior of Stokes profiles with B. First a weak field regime (B lower than 1200 G). The I component does not show any change in this first interval and the profiles V, U and Q appear.

The circular profile, V, increases its height when the magnetic field intensity is increased. In this regime of weak magnetic field, the height of the peaks in this profile is linearly proportional to the field intensity, B. Both Q and U grow quadratically with B for small magnetic field strengths. (see for instance Landi Degl'Innocenti & Landi Degl'Innocenti, 1973 or Landi Degl'Innocenti, 1994). The U profiles changes its shape from two to one lobe. Lastly, the Q component has three peaks and their shape has no change with the field. They only increase their height (also in the regime of strong magnetic field).

The strong field regime in our study includes the 2000 and 3000 G cases, In Stokes I it is possible to distinguish the formation of the two σ components and the central π component (remember: circular and linear polarized, respectively) with 3000 G, while for 2000 G these components start to be distinguished. The two σ components can also be observed in the U profile for these fields, the circular components are clearer but the central peak associated to the linear component does not change.

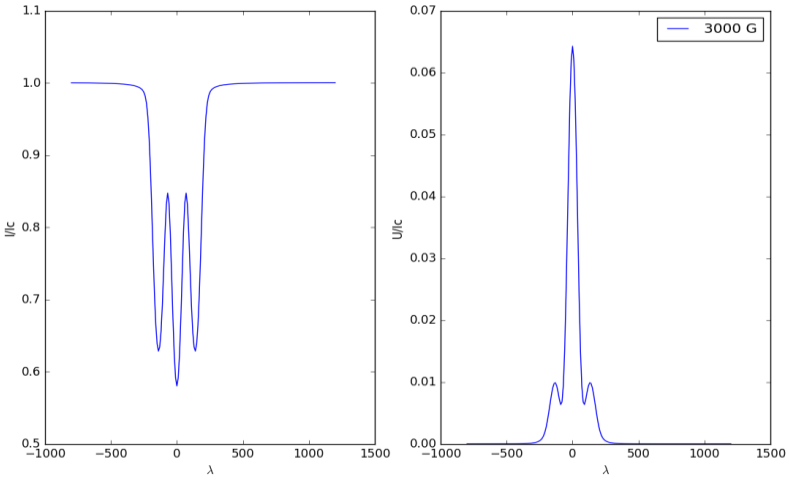

Figure 8. The profiles I and U at 3000 G. The σ components are now visible.

If we study the behavior of Stokes *V* when we change the magnetic field. In the regimen of strong magnetic field, we can see that when magnetic field strength is higher than 2000 G (see figure 9), the two peaks of the V start to separate and other two lower peaks appear in the center of the profile.

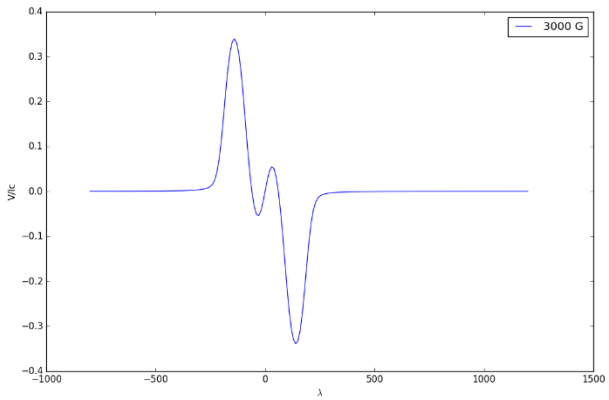

Figure 9. Profile V at 3000 G with the two peaks secondary peaks.

2.3 INCLINATION.

Now, it is the turn to study the changes of the Stokes profiles when the inclination of the magnetic field is changed. We are going to work with the base temperature in the VALC model, an intensity of 500 G and an azimuth of 0º.

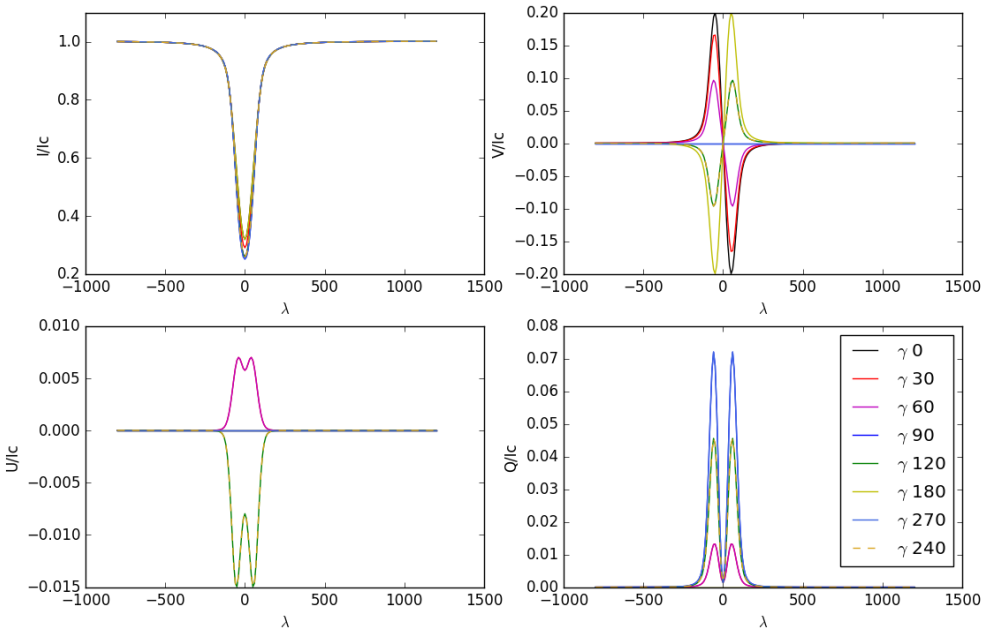

Figure 8. Stokes profiles normalized to the continuum intensity Ic with various values of inclination γ.

Starting with the profile I, we do not observe significant variations when we change the magnetic field inclination.

In the case of the profile V, the line is null when $\gamma = 90$ or 270. If we look at the expressions for the absorption matrix in the RTE (eq. 10 and 11) the elements ρ_U and $\eta_U$are always zero, and in this case the elements ρ_V and η_V are also zero. So, the absorption matrix takes the form:

$$K = \begin{pmatrix} \eta_I & \eta_Q & 0 & 0 \\ \eta_Q & \eta_I & 0 & 0 \\ 0 & 0 & \eta_I & \rho_Q \\ 0 & 0 & -\rho_Q & \eta_I 0 \end{pmatrix} \tag{15}$$

It is easy to see in the RTE (eq. 9) that the component $V$of the Stokes vector will be zero in this case.

When $\gamma = 0$ or 180 the V line is maximum, ρ_Q and η_Q are zero and ρ_V and η_V are maximum. The absorption matrix has this form:

$$K = \begin{pmatrix} \eta_I & 0 & 0 & \eta_V \\ 0 & \eta_I & \rho_V & 0 \\ 0 & -\rho_V & \eta_I & 0 \\ \eta_V & 0 & 0 & \eta_I \end{pmatrix} \tag{16}$$

As ρ_V and η_V are maximum the component V in the Stokes vector will be also maximum.

For other inclination angles we find an intermediate behavior. Moreover, as the elements of the matrix depend on the cosine and the square of the sine of inclination the line with 120º will be symmetric to the 240º one, for example, and antisymmetric to the lines with a relation of 180º (in the plot we observe that the line of 30º is antisymmetric to the line of 240º).

The next step is to analyze the U component. As we have already seen, with angle of azimuth $\chi = 0$ fixed, the ρ_U and η_U are always zero. So, we can only observe lines in the U profile due to the elements of crosstalk with the components V and Q, ρ_V and ρ_Q. This happens in the intermediate angles (30º, 60º, 120º, 240º) with the symmetries which we have already commented.

Finally, in the case of Q profile we observe that the it is maximum when the elements ρ_Q and η_Q are maximum, i.e. $\gamma = 90º$ or $270º$. In this case the absorption matrix takes the form of the eq. 15. In the same way, these profiles are null with $\gamma = 0$ or 180. The absorption matrix becomes like that of eq. 16 and thus, the Q component must be zero.

2.4 AZIMUTH.

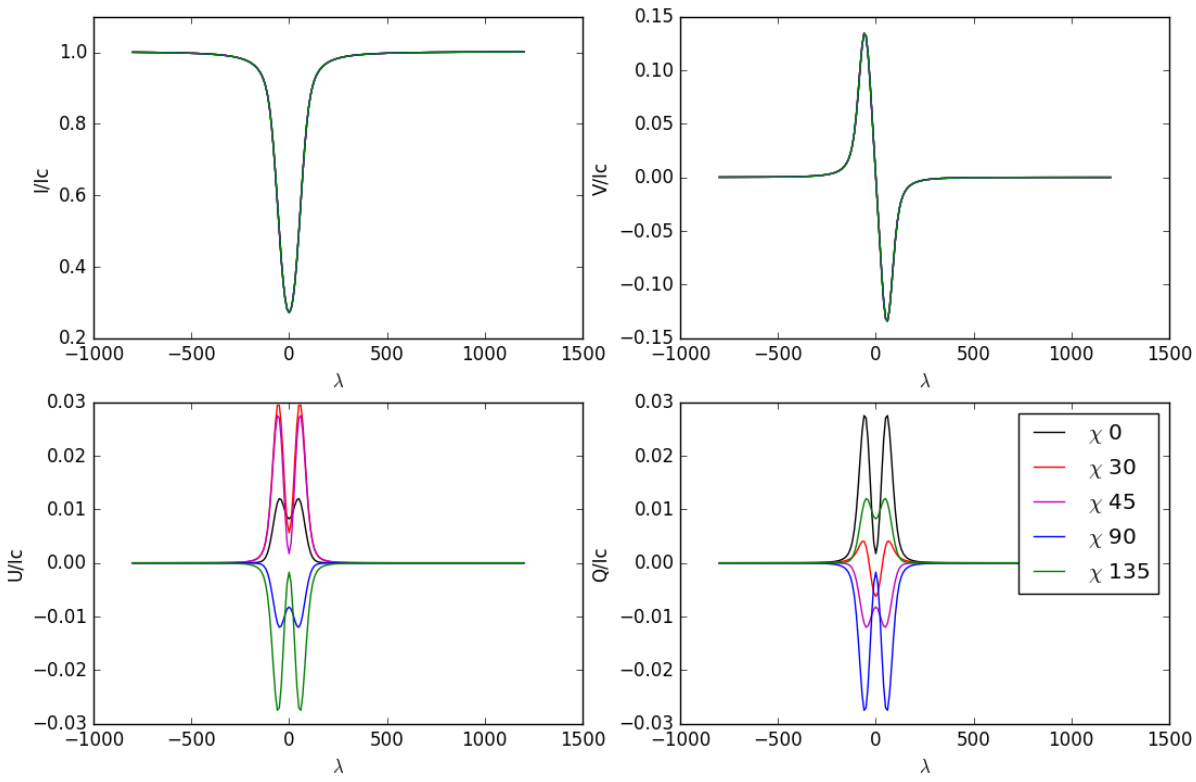

Figure 9. Stokes profiles normalized to the continuum intensity Ic with various values of azimuth χ.

In this section, in analogy with the previous one, we are going to keep the initial temperature of the model constant, a magnetic field intensity of 500 G and an inclination of 45º.

Stokes I does not suffer any change when we vary the azimuth. In the profile V, we cannot observe any change with the azimuth, either. We can explain this if we look at the elements ρ_V and η_V of the absorption matrix, they only depend on the inclination γ.

Th next step is to analyze the U and Q component in the extreme cases. If we look at the eq. 9 the dependence with the azimuth is cos2χ or sin2χ, so we are going to study the angles that make 0 or 1 the sine and the cosine.

When $\chi = 45^{o}$ or 135^{o}, $\sin 2\chi = 1$ and $\cos 2\chi = 0$. With this condition, the elements η_U and ρ_U are maximum and, η_Q and ρ_Q are null. The absorption matrix takes the form:

$$K = \begin{pmatrix} \eta_I & 0 & \eta_U & \eta_V \\ 0 & \eta_I & \rho_V & -\rho_U \\ \eta_U & -\rho_V & \eta_I & 0 \\ \eta_V & \rho_U & 0 & \eta_I \end{pmatrix} \quad (17)$$

As the terms η_Q and ρ_Q are null, the Q profile will be minimum. It is not null because in this case the elements η_V and ρ_V are not 0 and, in consequence, introduce crosstalk betwee V and Q anr/or U, i.e., along the atmosphere, a fraction of the circular polarized radiation it is transformed to linear polarized one This phenomenon it is known as Faraday rotation. In the case of the profile U, the elements η_U and ρ_U are maximum and we could expect that the profile is also maximum but, if we study the plot we can observe that the line of 30^{o} is a bit higher than the line of 45^{o}. A reason for this is that with 30^{o} all the elements of the absorption matrix are different to 0, and the sum of all the crosstalk elements is higher than the maximum value of η_U and ρ_U.

In the opposite case, when $\chi = 0^{o}$ or 90^{o} $\sin 2\chi = 0$ and $\cos 2\chi = 1$, the elements η_U and ρ_U are zero and η_Q and ρ_Q are maximum. In this situation, the absorption matrix is:

$$K = \begin{pmatrix} \eta_I & \eta_Q & 0 & \eta_V \\ \eta_Q & \eta_I & \rho_V & 0 \\ 0 & -\rho_V & \eta_I & \rho_Q \\ \eta_V & 0 & -\rho_Q & \eta_I \end{pmatrix} \quad (18)$$

Now, the profile Q is maximum because elements η_Q and ρ_Q are also maximum. In the profile U the lines of 0^{o} and 90^{o} are minimum but not zero due to the crosstalk elements as in the previous example.

2.5 VELOCITY.

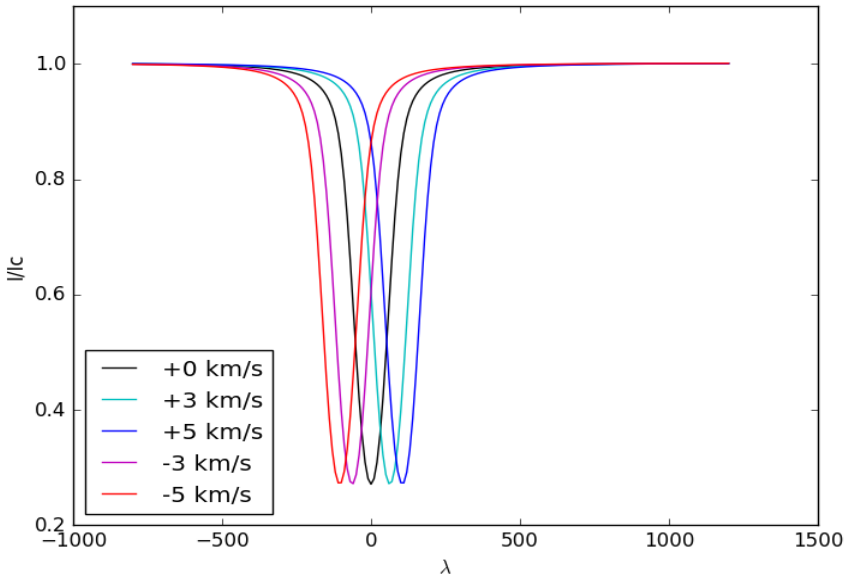

Figure 10. I profile normalized to the continuum Ic with different velocities of the source between -5 and 5 km/s.

Finally, we are going to study the effect in the profiles of the plasma velocity in the direction of the observer. We define the velocity as positive when the source is coming to the observer and negative when it is moving away.

We can observe that when the velocity is positive the line is the same but displaced to a greater wavelength, i.e, to the red (this is why this phenomena is known as a redshift) and when the velocity is negative the line is blueshifted, i.e., it is displaced to a lower wavelength. The effect in the profiles V, U and Q is the same.

This effect is described by the Doppler Effect, that gives us the change in the wavelength of a wave when the source and/or the observer are in motion. In this case, we can suppose that the observer is static and the Doppler Effect can be represented as:

$$\Delta\lambda = \lambda_0 \frac{v}{c} \tag{19}$$

Where λ_0 is the wavelength we are observing, v the line-of-sight component of the source (the photosphere surface in our case), and c the speed of light.

3. SUNSPOT STUDY WITH DATA FROM HINODE.

Estudiamos los datos obtenidos por el satélite japonés Hinode de una región activa de la fotosfera con una mancha solar de gran tamaño. La información obtenida en el capítulo anterior sobre a variación de los perfiles de Stokes frente a diferentes valores de temperatura, de intensidad, inclinación y azimut del campo magnético y de velocidad en la línea de visión del plasma nos servirá para identificar algunas de las características tanto de la mancha solar como de la granulación en el Sol en calma. De esta forma los perfiles de Stokes obtenidos por Hinode nos permitirán estructuras interesantes como la existencia de un campo magnético de gran intensidad en las regiones de la umbra o que la granulación es una manifestación de movimientos de convección bajo la superficie de la fotosfera.

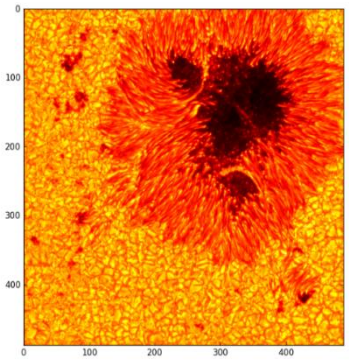

Figure 11. Representation of the normalized intensity (I/Ic) in the sunspot.

In this chapter, we are going to use data taken with the spectropolarimeter SP on board of the japanese satellite HINODE (Lites et al. 2001; Kosugi et al. 2007). The observed region includes the active region NOAA 10953 which, during the observations (2007 Apr. 30), was at an average heliocentric angle of $\theta = 12.8°$, i.e., very close to the disk center. This active region has recently been analyzed by Ruiz Cobo and Asensio Ramos (2013). The region was scanned in approximately 1000 steps, with a step width of 0."148 and a slit width of 0."158, recording the full Stokes vector of the pair of the neutral iron lines at 630 nm with a spectral sampling of 21.46 mÅ. The spatial resolution was approximately 0."32. The integration time was 4.8 s, resulting in an approximate noise level of 1.2×10^{-3}.

In the upper image, we observe a representation of the intensity information given by this data

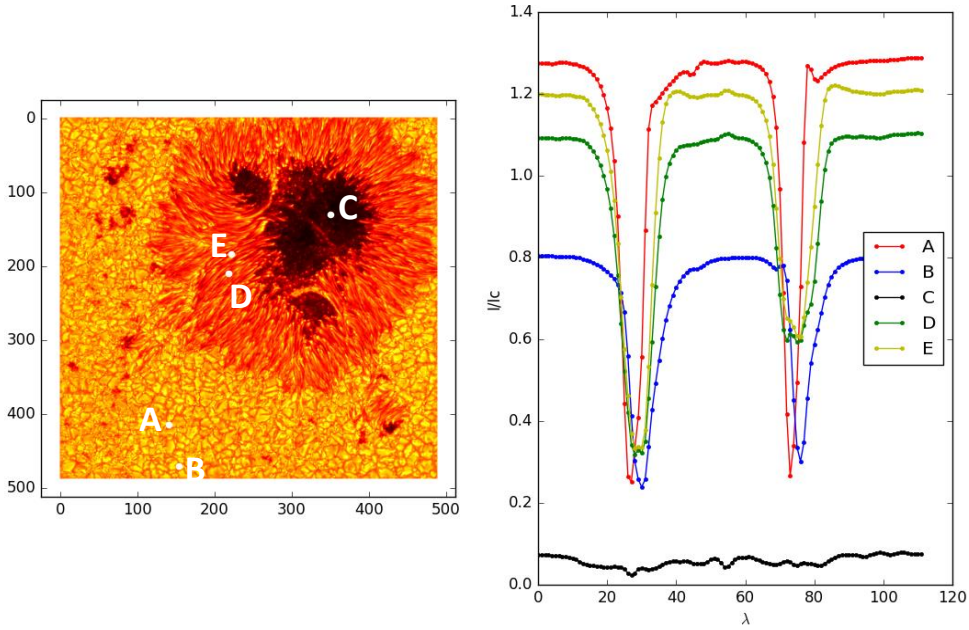

Figure 12. On the right are represented the I profiles normalized to the continuum Ic for different positions. On the left these positions are labelled: A and B correspond to quiet Sun regions; C to the umbra; and E and D to the penumbra.

In the first place, we look at the I profiles forming in different zones of the sunspot region. In the figure 14 the chosen zones and the resulting lines are shown. If we approximate the Sun like a black body, for a given wavelength the intensity will be higher when the temperature is also higher. Using this approach, we can determine the temperature of the different zones.

When we compare the point A, representative of granules, with the point B, the intergranule, we observe that the continuum is higher in A than in B. According to the black body assumption, this means that the temperature is higher in the granule and cooler in the granule. This result is in accordance with the theory of the granulation seen in section 1.1, the granules are sections of hot plasma moving upwards and the intergranule harbors cooled downwards-moving plasma. The level of the continuum shows this difference of temperatures.

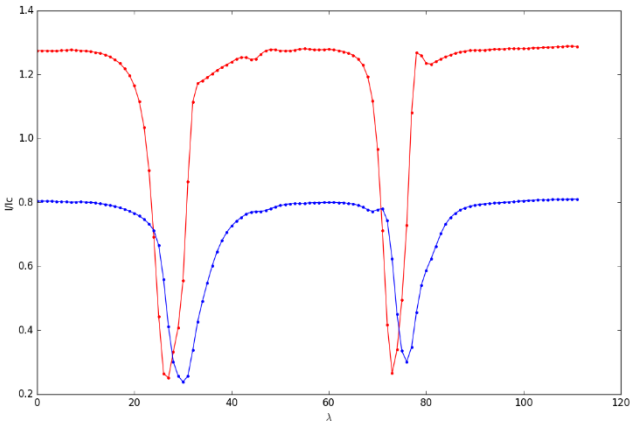

Figure 13. Stokes I profiles from the two points in a quiet Sun region. We can observe a shift in wavelength due to the different velocity of the line-of-sight velocity.

Focusing on the Stokes *I* profiles A and B (figure 15) we can observe how the peak of the first one (A, red line) is displaced to the left (i.e. it is blueshifted) respect to the second one (B, blue line). As we comment in section 2.5 this shift in wavelength is due to the Doppler effect produced by the different line-of-sight component of the velocity of the plasma at each position. We observe that in the granules the peak is at a lower wavelength, so the plasma in this zone must be moving upwards. In the intergranules the peak is in a higher wavelength and this means that the plasma is now moving downwards. In conclusion, with the information of the intensity in the continuum and the shift in the wavelength, we have an evidence of the convective motion just under the solar surface.

Now, if we look at the Stokes *I* profile of the pixel C, in the umbra, the most significant characteristic is its low intensity. As we explain in section 1.2, the temperature in the umbra of a sunspot is much lower than in the quiet sun (about 4000 K versus 5700 K), this is in accordance with the low value of the intensity that we have in this zone.

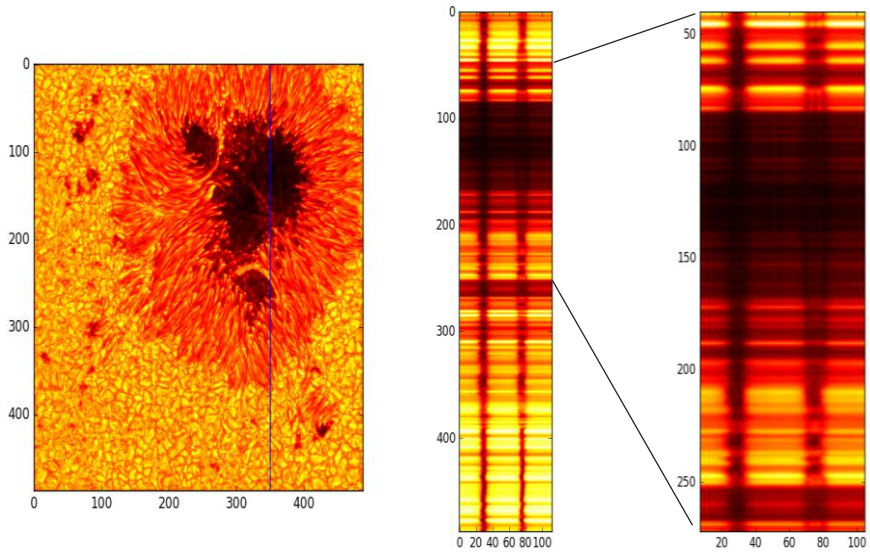

Figure 14. The vertical line on the left marks the position of a slit, which Stokes I spectrum is represented on the right panels. In these, the horizontal axis runs for wavelength, and the vertical for pixels along the slit. Darker colors indicate lower intensities.

The *I* profile in the umbra is very weak and it is difficult to distinguish the Zeeman components. In order to illustrate the apparition of the σ and π component we represent the variation in the intensity in a vertical line. Now we can observe that in the region of the umbra when the intensity is lower (darker in the plot), three lines appear. The central one is the π component and at its side there are the two σ components.

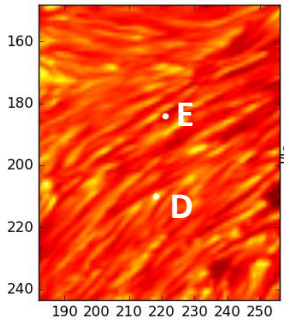

Figure 15. Position of the points D and E in the penumbra. The point D is in a brigth zone and the E in a dark one.

Also, in the case of the penumbra, we take two different points: D point in a bright zone of the penumbra and the point E in a dark one. As we can expect the intensity is higher in D than in E, but lower than in a granule. The temperature in E is lower than in the intergranule but higher than in the umbra. The explanation of the temperature of the penumbra is still an open problem (see for instance Ruiz Cobo and Asensio Ramos 2013), but it must be related with a change of the convention regime.

Now, we are going to study the V profile in the different zones.

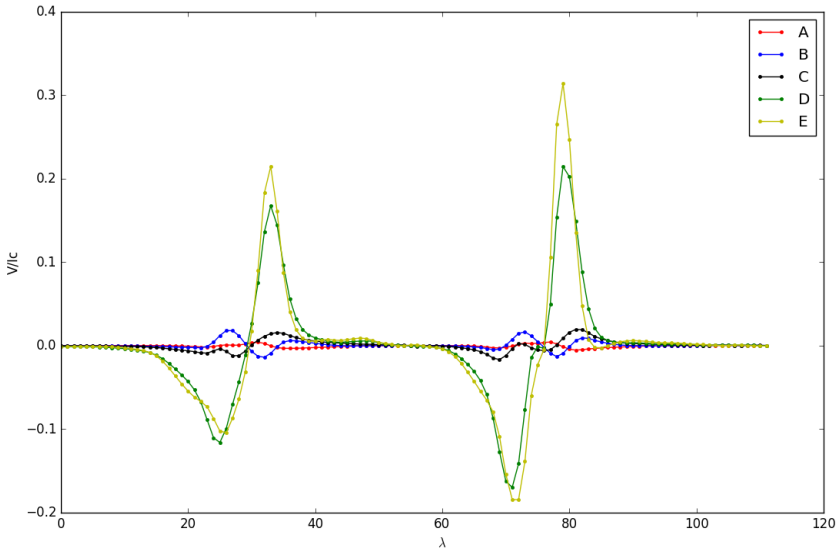

Figure 16. V profiles normalized to the continuum Ic from the five points selected in figure 14.

The first significant characteristic is that Stokes V for both pixels at qiet Sun and the one at the umbra are close to 0. In the case of quiet Sun the magnetic field is weak, and for that reason, Stokes V is very small (in section 2.2, we saw that when the magnetic field intensity is weak the profiles V, U, Q are also very weak). In the umbra, we could expect the presence of an important V profile but we cannot observe it. As we see in section 1.2, the magnetic field in the umbra has an inclination almost perpendicular to the solar surface. We can explain that if we take into account that the continuum intensity at the umbra it is very small, and consequently we have less photons. For this reason, the spectral line, which it is splitted in right and left circular polarized component, it is very

weak, resulting in small V profiles. In any case, we can see that the magnetic field is very intense because Stokes V it is completely splitted (see black lines in Figure 18)

The next step is to study the lines forming in the penumbra. We observe that the two profiles are very similar and more intense than the profiles of other zones. Even taking into account that inclination in the penumbra is close to 90 (because here the magnetic field is almost paralel to the solar surface and we are observing close to the disc center) and consequently Stokes V should be small, we observe a strong strong signal because we have many photons (the continuum intensity around 75% of that of the quiet Sun) and we have an intense magnetic field (tipically around 1500 G).

Now, it is the turn to analyze the Q and U component.

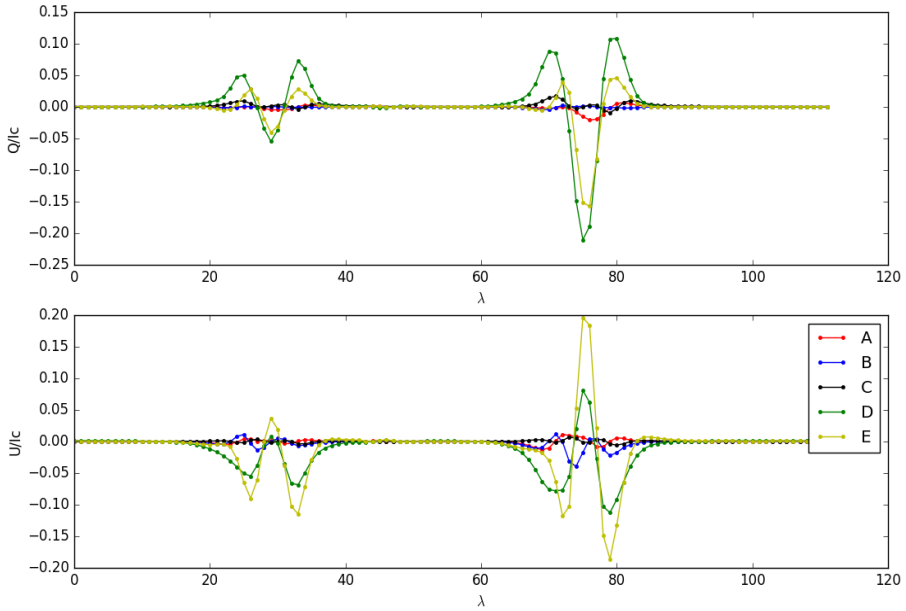

Figure 17. Q and U profiles normalized to the continuum Ic for the five points selected in figure 14.

Starting with the profiles of the zones of calm Sun we observe that, like in the case of the V profile, the lines are almost null. The intensity in the quiet Sun is weak and, in consequence, the parameters Q, U and V are nearby to 0.

As we said previously, the magnetic field in the region of the penumbra is parallel to the solar surface and the linear polarized light reach its maximum. Depending on the azimuth value we will have an important value of Q or U. In the case of this observation the zero of the azimuth is in the horizontal direction and as the magnetic field in the penumbra is mainy radial, in points D and E we will have an azimuth of around 200-300 degrees.

In Figure 20 we have plotted Stokes V, Q and U at the umbra. We can appreciate that both peaks of the line at 6302 Angstroms (more sensitive to the magnetic field) are completely separated, and consequently we can conclude that we are in the strong field case (see section 2.2).

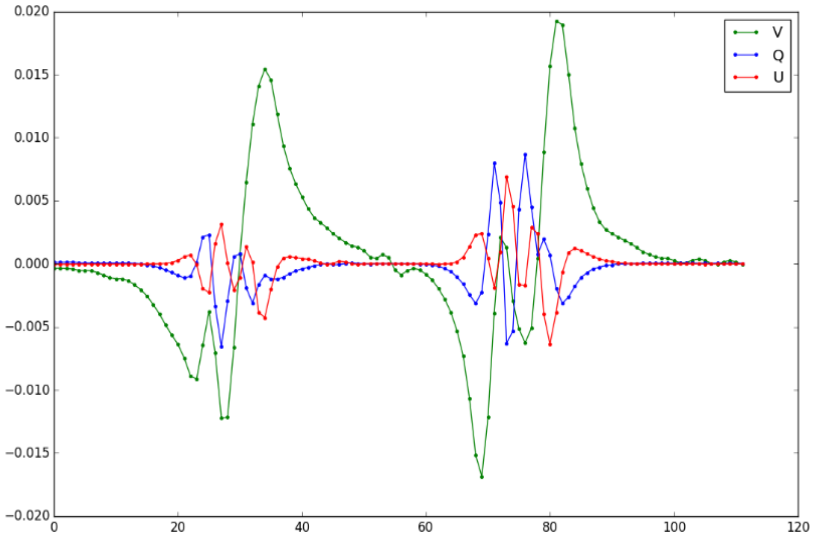

Figure 18. Detail of the profiles U, Q and V for the umbra

4. APPLICATIONS.

A partir de los datos de Hinode analizados en el capítulo anterior y aplicando dos aplicaciones sencillas calcularemos dos mapas de temperatura de velocidad en la línea de visión en la región de la mancha solar. Observamos como los valores de temperatura y velocidad están de acuerdo con lo visto en la introducción del trabajo. Además, los mapas serán útiles para mostrar la correlación entre las zonas de mayor temperatura con la presencia de material ascendente en los granulos y de temperaturas más bajas con material descendente en los intergranulos. De esta forma se muestra la relación de la granulación con el movimiento de convección bajo la superficie de la fotosfera.

In this chapter, we will use the data from Hinode to calculate an approximation to the temperature and line-of-sight velocity map in the region of the sunspot.

4.1 Temperature map.

Now, we are going to build a map with the distribution of temperature in the zone of the sunspot. The mean continuum intensity can be approximated by the Planck function evaluates at a temperature equal to the effective temperature of the Sun (5778 K). Consequently, in first order, we can approximate the fluctuations of the contrast as the derivative of the Planck function times the temperature fluctuations. The next development is only a first approximation, but it can help us to obtain some interesting results.

The contrast is defined as: $\frac{I_c-\overline{I_c}}{\overline{I_c}}$, where $\overline{I_c}$ represents the mean value of the continuum. Additionally, we can approximate the intensity as the intensity of a black body $I_\lambda \sim B_\lambda(T,\lambda)$, which can be defined with the Planck Law:

$$B_\lambda(T,\lambda) = \frac{2hc^2}{\lambda^5}\frac{1}{e^{\frac{hc}{\lambda k_B T}}-1} \tag{20}$$

Where h is the Planck constant, k_B, the Boltzman constant and c the speed of light.

Now we can express the contrast in function of $B_\lambda(T,\lambda)$:

$$\frac{I_c-\overline{I_c}}{\overline{I_c}} \sim \frac{\delta I_c}{\overline{I_c}} = \frac{\frac{dI_c}{dT}\Delta T}{\overline{I_c}} = \frac{\frac{dB_\lambda}{dT}\Delta T}{B_\lambda} = \frac{dlnB_\lambda}{dT}\Delta T \tag{21}$$

So, we can define the variation in the temperature as:

$$\Delta T = \frac{\frac{I_c-\overline{I_c}}{\overline{I_c}}}{\frac{dlnB_\lambda}{dT}} \tag{22}$$

On the other hand, if we derivate the Planck Law respect to the temperature (where T is the mean temperature):

$$\frac{dB_\lambda}{dT} = \frac{2hc^2}{\lambda^5}\frac{1}{e^{\frac{hc}{\lambda k_B T}} - 1}\frac{hc}{\lambda k_B T^2} = B_\lambda \frac{hc}{\lambda k_B T^2} \tag{23}$$

Clearing:

$$\frac{dB_\lambda}{dT}\frac{1}{B_\lambda} = \frac{dlnB_\lambda}{dT} = \frac{hc}{\lambda k_B T^2} \tag{24}$$

If we substitute (24) in (22), we obtain:

$$\Delta T = \frac{\lambda k_B}{hc}\frac{I_c - \overline{I_c}}{\overline{I_c}}T^2 \tag{25}$$

Using this relation, we can evaluate the temperature fluctuations respect to its mean simply by evaluating the fluctuations of intensity, and taking T=5778 K, and lambda=6301 Å.

This method provides us the following result:

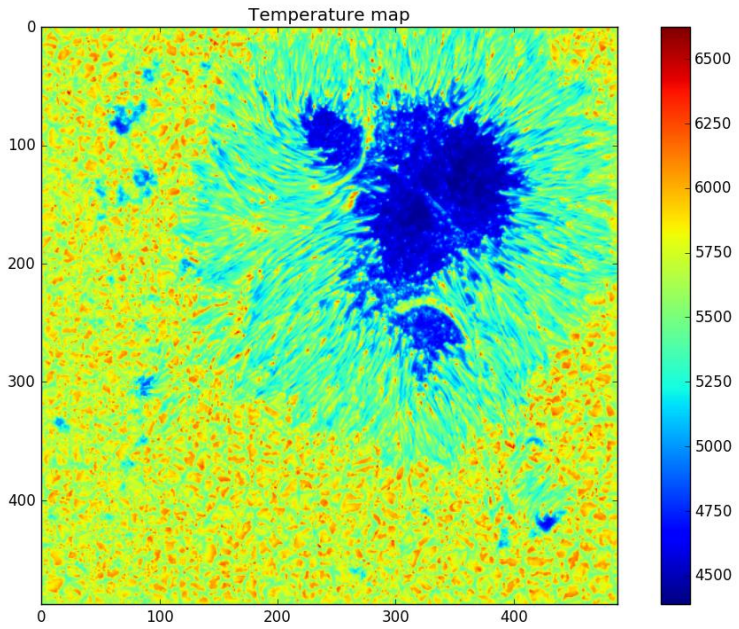

Figure 19. Temperature map in the sunspot region. The temperature is in Kelvin.

In the temperature map, we can observe some of the characteristics we have commented in previous sections. The temperature in the umbra is lower than in the other regions of the Sun, between 4750 and 4400 K. In the penumbra, the temperature values range from 5000 to 5500 K. The quiet Sun has higher temperatures, with important variations between zones. The coldest has a temperature around 5500K and the hottest one around 6200 K. This distribution of velocities is due to the convection under the surface of the Sun, as we have previously explained.

The next table, shows the temperature for the points used in chapter 3.

REGION	TEMPERATURE (K)
Quiet Sun (A)	6179
Quiet Sun (B)	5490
Umbra (C)	4419
Penumbra (D)	5147
Penumbra (E)	5410

The temperature results agree with the behavior of the continuum intensity for each case. The values also agree with the theory presented in the sections 1.1 and 1.2.

4.2 Velocity map.

In this final section, we are going to use the shift in the wavelength of the minima of the spectral lines to make a map of the line-of-sight velocity of the plasma in our image.

As we saw in section 2.5 the Doppler effect for a static observer takes the form of eq. 19. From this expression, we can obtain the component of the velocity along the line of sight (usually called V_{LoS} or line-of-sight velocity) in function of the shift of the minimum of the line ($\Delta\lambda$) and the wavelength at rest of this line, λ_0:

$$v = c\frac{\Delta\lambda}{\lambda_0} \tag{23}$$

So, we can calculate the shift of the minimum of the line as the distance between the minimum of the line for every pixel and its average (we will suppose that the average line-of-sight velocity is zero). We adopt 21.46 mÅ as the spectral sampling of the spectropolarimeter SP/Hinode. Now, we have the variation in wavelength and we can calculate the line-of-sight component of the plasma velocity in each point.

The result is represented in the next velocity map:

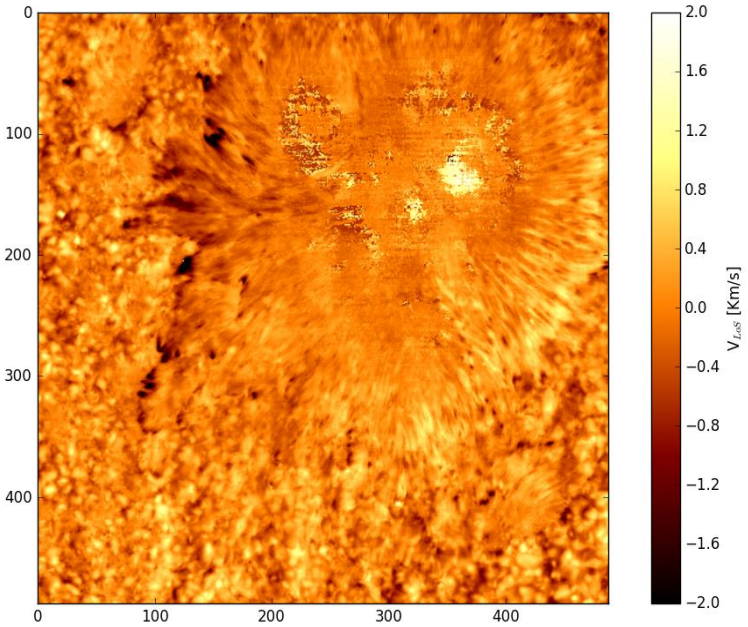

Figure 20. Velocity map in the sunspot region. The velocity is in Km/s and positive values of the velocity in this figure correspond to up-ward (blueshift) motions

Taking into account that in the quiet Sun we are observing the effect of convection, it would be expected a better correlation between that maps of temperature and velocity in the quiet Sun regions. The explanation of this discrepancy can be that our methods ignores some detail:

- The velocity is measured from the position of the minimum of the line so, we are calculating the velocity at higher layers than the temperature, because the minimum of the line forms always at higher layer than the continuum.
- The Sun has other velocity fields apart from the velocity produced by the convection. Some constant fields, like the rotation of the Sun or the relatively motion between the Sun and the Earth, and other components that vary in each pixel produced by the vibration of the solar surface (p-mode of sound waves with a frequency of 5 minutes). These velocities contaminate our result (Stix, 2002).

In spite of these problems, we can appreciate some interesting structures in the velocity field in the sunspot. In the umbra, the velocity is slightly negative (the plasma is descending) although theoretically it should be nearly at rest (Stix, 2002). We observe in this region zones of strong upwards velocities, these are the regions of stronger magnetic field and, in consequence, the core of the line strongly departure from a parabola a (due to the Zeeman splitting it has three peaks) and our method fail. In the penumbra, we observe a positive velocity: taking into account that plasma is frozen (Alfvèn theorem) the motion should follow the field lines and we know that in the penumbra this field lines are nearly parallel to the surface. This implies that the line-of-sight velocity field we are observing is the vertical component of a strong velocity field. In fact, there is a radial velocity field of around 6 km/s along penumbra filaments known as Evershed effect (see section 1.2).

Even despite the problems mentioned before, it still possible to observe a slight correlation between higher temperature regions and upwards motions (the zones of higher temperature coincide with zones of positive velocity The line-of-sight velocity in this region is around 1.12 Km/s in the bright zones (granules) and -0.5 Km/s in the dark zones (intergranules), this result agree with the values given in section 1.1.

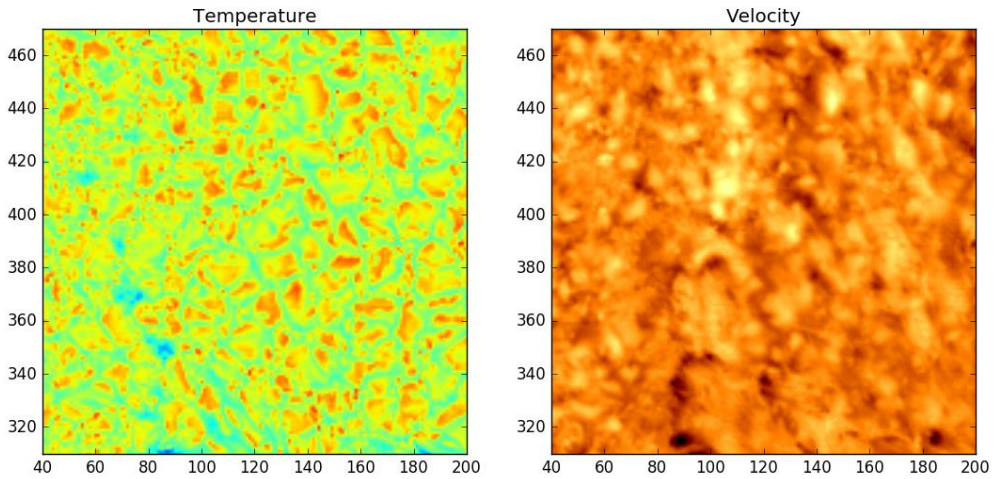

Figure 21. Temperature and line of sight velocity maps in a quiet Sun region.

5. CONCLUSIONS.

In this work, we have studied the effects of the changes in temperature and in the magnetic field on the Stokes parameters and we have used this knowledge to study real observational data.

We have used the SIR code to obtain how the Stokes profiles of a pair of Fe I lines change after variations of different physical quantities. We observed the effect of temperature, magnetic field strength, inclination and azimuth of the magnetic field and plasma velocity on the Stokes profiles. From this study, we could collect some interesting results which provided very relevant information to analyze real data. The relations between the continuum intensity and the temperature (the continuum is higher when we increase the temperature) and between the position of the line minimum with the velocity (Doppler effect) were necessary to calculate the maps of temperature and velocity. In relation to the magnetic field, we observed its effect on the polarized components; we have paid special attention to the behavior of Stokes V for weak and strong fields, and the importance of both approaches to determine the magnetic field strength. When we analyzed the effect of the inclination and azimuth, we could determine the angles that produce null or maximum profiles and, also, we observed the relevance of the crosstalk terms from the absorption matrix in the lines formation.

With all this information, we could study a set of real data, in particular we have used Stokes observations taken by the spectropolarimeter SP on board of the Hinode satellite. The data consist on observations of two photospheric Fe I lines at 630.1 and 630.2 nm for an active region containing a big sunspot. We achieved some conclusions that illustrate interesting phenomena predicted by the theory presented in the introduction. The shape of Stokes U, Q and V proved that the magnetic field in the penumbra and umbra is stronger than in the quiet Sun. Besides, with the shape of these profiles, we can obtain some qualitative information about the inclination of the magnetic field, for example, that, while in the umbra the field is almost perpendicular to the solar surface (strong V profiles), in the penumbra it is nearly parallel to the solar surface (strong Q and U profiles). In the quiet Sun, we could observe some differences in the level of the continuum and in the position of the minima of the lines between the bright and dark zones. This correlation between temperature and velocity is in good agreement with the convective character of the solar granulation.

Finally, in chapter 4, we applied two simple approaches that allow us to obtain information of temperatures and line of sight velocities of the photosphere from Hinode data. First, we used the relation between the continuum level and the temperature to calculate a temperature map that showed the lowest temperature in the umbra and the variations of the temperature in the quiet Sun due to the convection. Furthermore, using the Doppler effect, we obtained a map of the line-of-sight component of the velocity. The approach that we have used is not valid in the umbra, because there, the Stokes I profiles appear splitted in several component and the parabolic fit to the minimum of the line does not work. However, in the quiet Sun region this method produces good results, in particular we showed the difference of velocities in the granulation and the correlation between brighter zones, higher temperature and positive velocities in the granules, versus darker zones, lower temperature and negative velocities in the intergranules.

An interesting continuation to this work could be to improve the methods for calculating the maps of temperature and velocities reducing the errors and eliminating the

elements that contaminate the data. Also, we could attempt to obtain the value of the magnetic field strength, inclination and azimuth in the region of the sunspot.

In conclusion, in this work we have seen the possibilities that the analyses of the polarized light give us to improve our knowledge about the solar photosphere. Besides, we can demonstrate some of the most relevant characteristics of the sunspots and the granulation thanks to the Hinode data, showing the possibilities of the spectropolarimetry.

REFERENCES

Bellot Rubio, L. R. 1998. Structure of solar magnetic elements from the inversion of Stokes spectra. Tesis doctoral. Insituto de Astrofísicia de Canarias

Bellot Rubio, L.R. 2003, Inversion of Stokes profiles with SIR, (Freiburg: Kiepenheuer-Institut für Sonnenphysik)

Gray, D. G. (1992). "The observation and analysis of stellar phostospheres", 2nd edition, CUP, Cambridge

Hecht, E. 1998. Óptica. Addison Wesley.

Kosugi, T., Matsuzaki, K., Sokao, T., et al. 2007, Sol. Phys., 243, 3

Landi Degl'Innocenti, E. & Landi Degl'Innocenti, M., 1973, Solar Physics, 31, 299

Landi Degl'Innocenti, E., 1994, in Solar Surface Magnetism. NATO Advanced Science Institutes (ASI) Series C: Mathematical and Physical Sciences, Proceedings of the NATO Advanced Research Workshop, Netherlands. Edited by Robert J. Rutten and Carolus J. Schrijver.

Lites, B. W., Elmore, D. F., & Streander, K. V. 2001, ASPC, 236, 33

Ruiz Cobo, B., & del Toro Iniesta, J.C. 1992, ApJ 398, 375

Ruiz Cobo, B., and Asensio Ramos, A., 2013 A&A 549, L4

Stenflo, J.O., 1985, Solar Phys. 100,189

Stix, M. 2002 "The Sun: An Introduction", Springer-Verlarg, Berlín

Vernaza J.E., Avrett E.H., & Loeser R., 1981, ApJS 45, 635

Figures:

Figure 1: https://www.nasa.gov/mission_pages/hinode/solar_013.html

Figure 2: https://en.wikipedia.org/wiki/Sunspot#/media/File:172197main_NASA_Flare_Gband_lg-withouttext.jpg

Figure 3: Bray and Loughhead, "Sunspots", Dover Publications, 1964

Figure 4: https://en.wikipedia.org/wiki/Stellar_magnetic_field#/media/File:ZeemanEffect.GIF